FAK is required for axonal sorting by Schwann cells

Matthew Grove,[1] Noboru H. Komiyama,[2] Klaus-Armin Nave,[3] Seth G. Grant,[2] Diane L. Sherman,[1] and Peter J. Brophy[1]

[1]Centre for Neuroscience Research, University of Edinburgh, Edinburgh EH9 1QH, Scotland, UK
[2]Wellcome Trust Sanger Institute, Hinxton CB10 1SA, England, UK
[3]Department of Neurogenetics, Max-Planck-Institute of Experimental Medicine, 37075 Göttingen, Germany

Signaling by laminins and axonal neuregulin has been implicated in regulating axon sorting by myelin-forming Schwann cells. However, the signal transduction mechanisms are unknown. Focal adhesion kinase (FAK) has been linked to α6β1 integrin and ErbB receptor signaling, and we show that myelination by Schwann cells lacking FAK is severely impaired. Mutant Schwann cells could interdigitate between axon bundles, indicating that FAK signaling was not required for process extension. However, Schwann cell FAK was required to stimulate cell proliferation, suggesting that amyelination was caused by insufficient Schwann cells. ErbB2 receptor and AKT were robustly phosphorylated in mutant Schwann cells, indicating that neuregulin signaling from axons was unimpaired. These findings demonstrate the vital relationship between axon defasciculation and Schwann cell number and show the importance of FAK in regulating cell proliferation in the developing nervous system.

Introduction

During embryonic development in the mammalian peripheral nervous system (PNS), bundles of growing axons are surrounded by Schwann cell processes (Jessen and Mirsky, 2005). These processes sort larger caliber axons to the periphery of the bundles, where they adopt a 1:1 relationship with Schwann cells and are myelinated (Sherman and Brophy, 2005). The transition to individual axon ensheathment is associated with, and presumed to depend upon, extensive Schwann cell proliferation (Martin and Webster, 1973; Webster et al., 1973; Stewart et al., 1993). Schwann cell proliferation during development is stimulated by cell surface axonal molecules, called the neuregulins, acting via ErbB receptors (Wood and Bunge, 1975; Salzer et al., 1980; Morrissey et al., 1995; Riethmacher et al., 1997). Laminins in the basal lamina secreted by Schwann cells have also been implicated in promoting Schwann cell proliferation at the early stage of axon sorting (Bunge et al., 1986; Yu et al., 2005). These stimuli may not be mutually exclusive because crosstalk between their signal transduction pathways occurs in oligodendrocytes in the central nervous system (CNS; Colognato et al., 2002).

Murine Schwann cells lacking the laminin γ1 chain lose all their known laminins and display reduced proliferation during sorting, increased postnatal apoptosis, and decreased ErbB2

phosphorylation (Yu et al., 2005). In contrast, the absence of laminin-2 and -8 influences proliferation and radial axonal sorting, but cell death is unaffected, at least up to 2 wk after birth (Wallquist et al., 2005; Yang et al., 2005). A major laminin receptor in the Schwann cell plasma membrane is α6β1 integrin (Previtali et al., 2003). Myelination in culture is blocked by anti–β1-integrin antibodies, and Schwann cells lacking β1-integrin display impaired radial sorting (Fernandez-Valle et al., 1994; Feltri et al., 2002). Nevertheless, neither the proliferation nor the survival of Schwann cells is affected in these mice, and they can go on to sort and myelinate axons, albeit inefficiently. Hence, the loss of different laminins and their receptors may have distinct effects during axon sorting.

We have investigated the signaling pathways that might regulate axon sorting. FAK is a nonreceptor tyrosine kinase that is central to several signal transduction pathways, including those that stimulate proliferation (Ilic et al., 1997; Geiger et al., 2001). FAK associates with β1 integrin in Schwann cells, and the presence of basal lamina activates FAK (Fernandez-Valle et al., 1998). Neuregulin also causes FAK to associate with the Schwann cell ErbB2–ErbB3 complex (Vartanian et al., 2000). Significantly, Schwann cells in mice deficient in neuregulin not only produce thinner myelin sheaths but also display defects in axon defasciculation (Michailov et al., 2004; Taveggia et al., 2005).

Constitutive inactivation of FAK is lethal (Ilic et al., 1995); hence, we have investigated the role of Schwann cell FAK by targeted deletion using the Cre-loxP system. We find that FAK

signaling in Schwann cells during axonal sorting is necessary to stimulate proliferation, and that without this late embryonic burst of cell division defasciculation of axons is highly impaired.

Results and discussion

Conditional inactivation of *Fak* in myelinating Schwann cells

We generated mice without functional FAK in myelinating Schwann cells, as described in Materials and methods. *Fak^flox/flox^/Cnp-Cre* mice were born in expected numbers, had no clinical phenotype at birth, and were of normal weight (wild-type, 1.39 ± 0.04 g; mutant, 1.37 ± 0.03 g; mean ± SEM; *n* = 3 each). Cre-mediated recombination in this *Fak^flox/flox^* mouse line has already been shown to prevent expression of either FAK or its truncated forms in the epidermis and in neurons derived from embryonic stem (ES) cells (McLean et al., 2004; Charlesworth et al., 2006).

First, we demonstrated Cre recombinase–mediated inactivation of *Fak* in mouse sciatic nerve during late embryonic development, when radial sorting of axons occurs. Genomic PCR analysis showed that Cre-mediated recombination at the *lox*P sites at embryonic day (E) 18.5 was very efficient (Fig. 1 A). This is consistent with the fact that the regulatory elements of the CNP gene are robustly active in all perinatal Schwann cells in the sciatic nerve (Yuan et al., 2002). The low level of PCR product corresponding to the residual unrecombined floxed gene probably originates from perineurial fibroblasts and some Schwann cells that escape recombination. The absence of FAK from most Schwann cells in mutant nerve was made clear by immunofluorescence (Fig. 1 B). In the case of those few Schwann cells in the mutant nerve that had ensheathed axons and went on to myelinate, it is possible that only one *Fak* allele had been inactivated because these cells were always positive for FAK by immunofluorescence (Fig. 1 C). By 2 wk after birth, *Fak^flox/flox^/Cnp-Cre* mice were distinctly less active than normal littermates, and they began to display a tremor by 3–4 wk that progressed to hindlimb paralysis after 3 mo in those few animals that were allowed to reach that age (Videos 1 [wild-type] and 2 [mutant], available at http://www.jcb.org/cgi/content/full/jcb.200609021/DC1).

FAK mutant Schwann cells associate normally with embryonic axon bundles

By E18.5, axons are organized into bundles and enveloped by Schwann cells (Martin and Webster, 1973; Webster et al., 1973). There were considerable variations in axon caliber and bundle size at this age, but no discernible differences between control and mutant nerves (Fig. 2, A–D). Furthermore, both control and mutant Schwann cells were able to extend processes into the bundles, showing that FAK-null cells could still initiate the first steps in axonal sorting (Fig. 2, C and D). To confirm that mutant Schwann cells interdigitated into bundles normally, we counted the number of Schwann cells with visible nuclei that were associated with bundles and determined the percentage that extended processes into bundles, and they were essentially identical in wild-type and mutant cells (wild-type, 97.9 ± 2.1%; mutant,
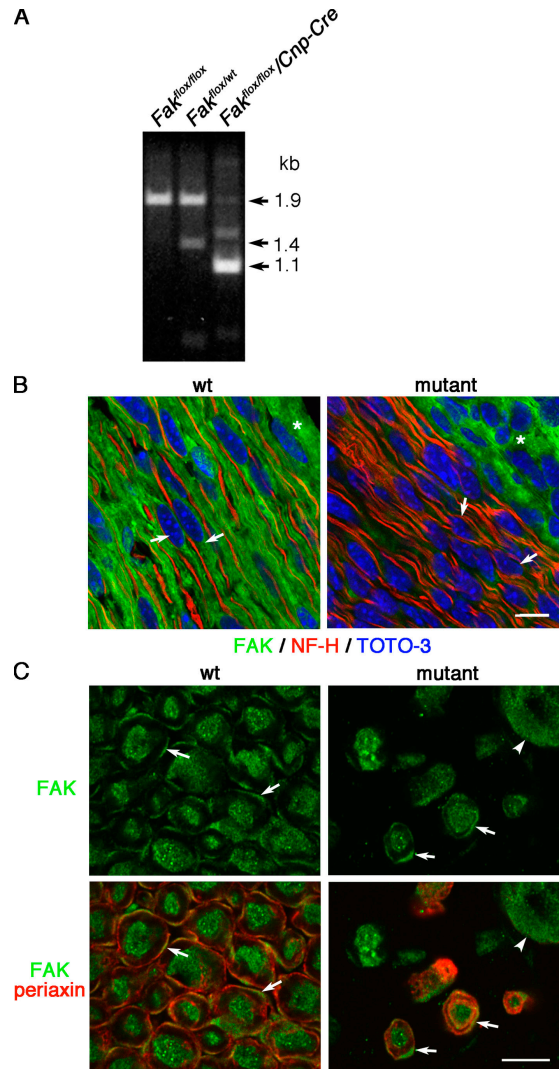

Figure 1. **Cre-mediated deletion of FAK in Schwann cells.** (A) Genotyping of sciatic nerve genomic DNA isolated from *Fak^flox/flox^*, *Fak^flox/wt^*, and *Fak^flox/flox^/Cnp-Cre* mice at E18.5 revealed highly efficient recombination at the *loxP sites* in the presence of Cre recombinase. After PCR amplification and digestion with HindIII, mice homozygous for the floxed allele showed a band in Agarose gel electrophoresis of 1.9 kb, whereas after recombination in the presence of Cre recombinase this band was shifted to 1.1 kb. Note that this was readily distinguishable from the product of 1.4 kb obtained from the wild-type allele in mice heterozygous for the floxed and wild-type allele (*Fak^flox/wt^*). The band at 1.5 kb in lane 3 is a genomic PCR artifact of variable intensity and no significance. (B) Immunofluorescence of longitudinal sections of sciatic nerves from P4 wild-type and mutant nerves shows that FAK (green) is expressed in wild-type Schwann cells (arrows) and in perineurial fibroblasts (asterisks) in both wild-type and mutant nerves, but is not expressed in mutant Schwann cells (arrows). Nuclear staining (blue) and immunofluorescence for neurofilament-H (NF-H, red) show the location of the axons associated with Schwann cells. (C) Immunofluorescence of transverse sections of wild-type and mutant tibial nerves from 3-mo-old mice shows that FAK (green) and Periaxin (red) colocalize at the plasma membranes of adult myelinating Schwann cells in both wild-type and mutant nerves (arrows). Note the strong staining for FAK in unsorted axon bundles (arrowhead). Bars, 10 μm.

98.6 ± 0.7%; mean ± SEM; *n* = 3 each). Schwann cells that had adopted a one-to-one relationship with axons were detectable in both control and mutant nerves (Fig. 2, C and D, arrowheads, and Fig. 1 C). Although loss of FAK has been shown to
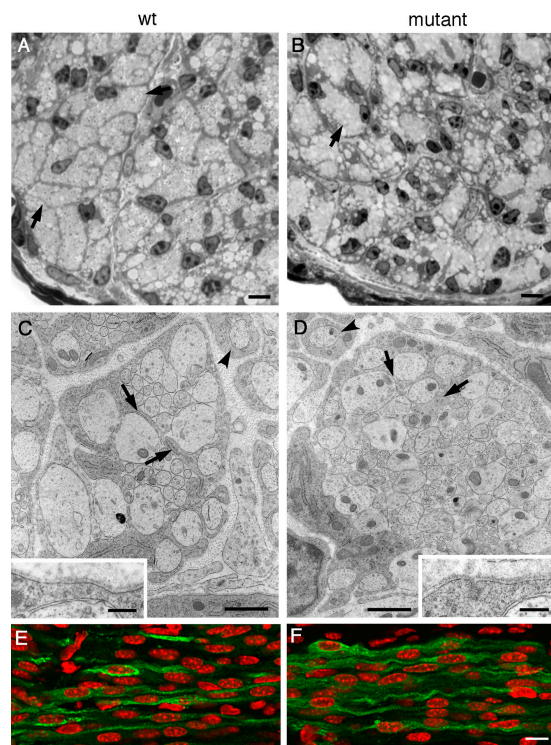
Figure 2. Embryonic FAK-null Schwann cells differentiate and associate normally with axon bundles. (A and B) Light microscopy of 1-μm transverse sections stained with toluidine blue from wild-type (A) and mutant (B) tibial nerve showed that bundles of axons (arrows) vary in size at E18.5, but mutant nerves do not display any abnormalities at this age. (C and D) Electron microscopy revealed that axon bundles with a range of axon calibers are interdigitated by Schwann cell processes (arrows) in both wild-type (C) and mutant (D) nerves. The insets show that basal lamina is apparently normal in mutant nerves (D) when compared with wild-type (C). C and D show that Schwann cells in a 1:1 relationship with axons are also detectable in both wild-type and mutant (arrowheads). (E and F) Immunofluorescence microscopy showed that by P1 Periaxin (green) had relocated from the nucleus (labeled with TOTO-3; red) to the cytoplasm in both wild-type (E) and mutant (F) Schwann cells. Bars: (A and B) 10 μm; (C and D) 5 μm; (C and D, insets) 0.2 μm; (E and F) 1 μm.

Figure 3. FAK is required for axon defasciculation. (A–F) By P3, radial sorting and ensheathment of axons by Schwann cells are highly impaired in the absence of FAK. Light microscopy of transverse sections of sciatic nerve shows that, unlike wild-type nerve, mutant nerves had many bundles of axons (arrowheads), and this lack of defasciculation is reflected in the smaller overall diameter of the mutant nerves (A and B). Higher power images show that large-caliber axons persisted in bundles in the absence of FAK, although there had been partial sorting of these axons to the edges of the bundles (D, arrowheads). In some cases, large-caliber axons were sorted to smaller bundles (D and F). In contrast, large-caliber axons in wild-type axons were mostly sorted away from axon bundles, leaving behind axons of lower caliber (E). It was still possible to observe interdigitating Schwann cell processes at the periphery of the bundles (F, arrow). Bars: (A and B) 15 μm; (C and D) 5 μm; (E and F) 1μm.

cause aberrations in basal lamina structure caused by altered laminin organization in the CNS (Beggs et al., 2003), basal lamina surrounding axon bundles in the wild-type nerve (Fig. 2 C, inset) appeared intact and identical to that in the mutant (Fig. 2 D, inset).

To confirm that mutant embryonic Schwann cells had differentiated, we analyzed the localization of Periaxin. Periaxin is first detectable in the nuclei of embryonic Schwann cells in the sciatic nerve, but relocalizes to the cytoplasm of Schwann cells around E17.5–18.5 (Sherman and Brophy, 2000). At postnatal day (P) 1, Periaxin was primarily cytoplasmic in both control and mutant nerves, indicating that mutant Schwann cells were not arrested in their embryonic development (Fig. 2, E and F).

FAK is required for Schwann cell proliferation and radial sorting of axonal bundles

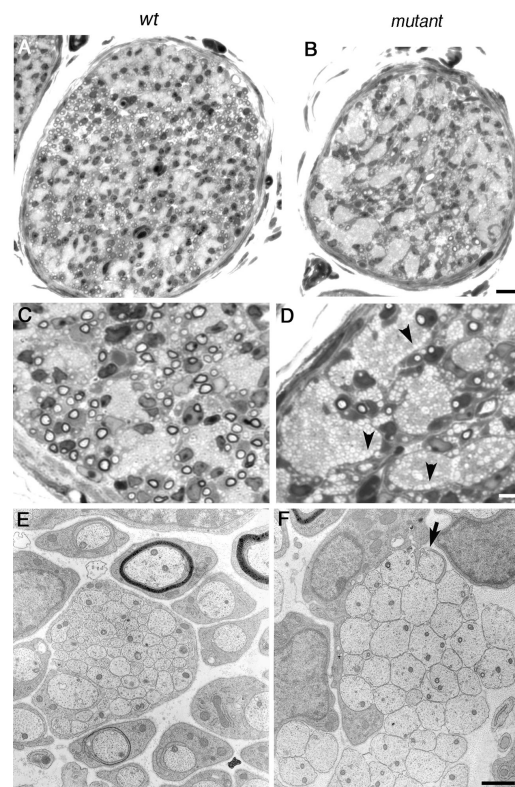Extensive axonal sorting and the establishment of a 1:1 relationship between Schwann cells and axons had occurred by P3 in control sciatic nerve (Fig. 3, A and C). Mutant nerves were considerably smaller in cross-sectional area than control nerves (wild-type, $13,405 \pm 640$ μm^2; mutant, $7,548 \pm 573$ μm^2; mean $\pm$ SEM; $n = 3$ each), which reflected the retardation of Schwann cell ensheathment at axons in the absence of FAK (Fig. 3, A and B). Axon bundles in mutant nerves remained larger, with much fewer ensheathed axons compared with control nerves (wild-type, 284 ± 26; mutant, 19 ± 3; mean $\pm$ SEM; $n = 3$ each; Fig. 3, C and D). In contrast to control axon bundles, where large-caliber axons were peeled off by Schwann cells, leaving behind axons with a range of diameters (Fig. 3 E), mutant nerves were characterized by the arrested sorting of large-caliber axons to the edges of the bundles (Fig. 3 D). This provided further evidence that mutant Schwann cells were capable of inserting processes into bundles and sorting axons radially. Subsequently, smaller bundles of large-caliber axons appeared to be sorted away from mixed bundles (Fig. 3 F); a similar phenomenon has been observed in β1 integrin–deficient nerves (Feltri et al., 2002).

Figure 4. **Reduced numbers of Schwann cells in mutant nerves.** (A) Mutant nerves have fewer Schwann cells per cross section of tibial nerve from E18.5. (B) Immunofluorescence and counting of labeled nuclei after BrdU incorporation shows decreased proliferation in mutant nerves. (C) Immunofluorescence for activated caspase-3 in the mutant shows no elevated apoptosis from E18.5 through P4 compared with wild-type. A rare caspase-3–positive cell is indicated by the arrow. (D) Western blot of P1 sciatic nerves showing that ErbB2 and AKT phosphorylation are unimpaired in the mutant. The loading control was β-actin. Values are means ± the SEM. n = 3 mice for each age. *, P < 0.05; **, P < 0.01 from paired t test. Bar, 30 μm.
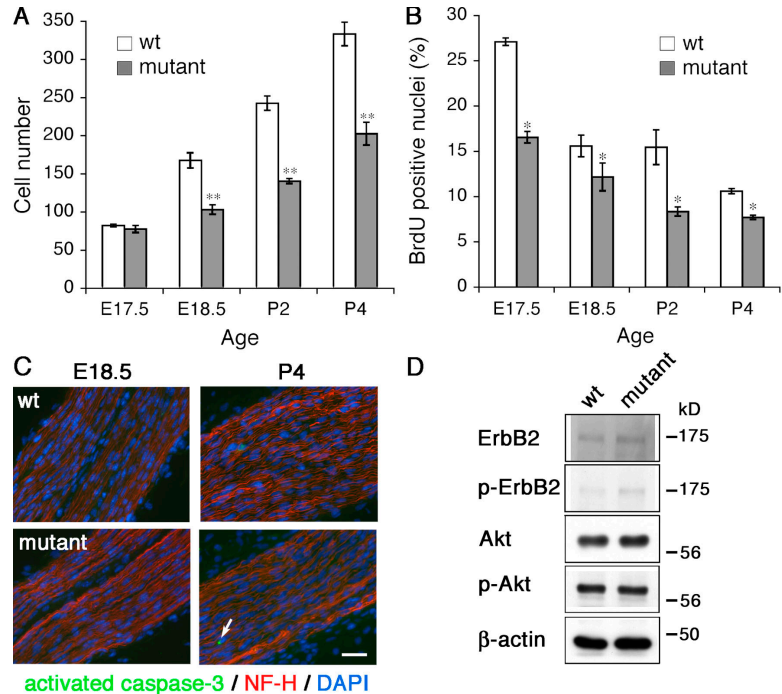
We asked if the abnormalities in axon sorting in the mutant might be caused by deficiencies in the number of Schwann cells. After E17.5, the number of cells in mutant nerves was significantly reduced in comparison to control nerves up to P4 (Fig. 4 A). This could be caused by decreased proliferation, increased cell death, or both. Labeling with BrdU revealed that Schwann cells lacking FAK proliferated much less than control cells from E17.5 to P4 (Fig. 4 B). FAK signaling can prevent apoptosis in vivo (McLean et al., 2004); nevertheless, there was no demonstrable increase in apoptosis in mutant nerves at either E18.5 or P4, as detected by activated caspase-3 expression, and activated caspase-3–positive cells always comprised <0.1% of all cells in wild-type and mutant nerves (Fig. 4 C). These results are in marked contrast to FAK deletion in the developing forebrain, where although neuronal apoptosis was unaffected, proliferation was also unaffected; in contrast, the absence of FAK affected cell migration in the CNS, probably because of alterations in basal lamina organization; furthermore, the morphology of neuronal dendrites was abnormal (Beggs et al., 2003). It seems that the effect of losing FAK depends very much on cell type. In a keratinocyte-restricted FAK knockout, the absence of FAK resulted in fewer keratinocyte precursors, which may be caused by defects in mitosis, although apoptosis was unaffected, whereas FAK-null keratinocytes proliferated and migrated normally (Essayem et al., 2006). Interestingly, these FAK-null keratinocytes undergo massive apoptosis if placed in culture, which underscores the importance of evaluating the consequences of deleting FAK in vivo when studying complex tissues.

Because signaling by axonal neuregulin via ErbB2–ErbB3 receptors has been linked to FAK recruitment (Vartanian et al., 2000), it was important to determine if any effects on radial sorting that we might attribute to loss of FAK were caused by aberrant ErbB2–ErbB3 function. Western blots showed that ErbB2 phosphorylation was not impaired in the mutant at P1, indicating that axonal neuregulin could still activate the receptor (Fig. 4 D). Furthermore AKT phosphorylation was also normal, indicating no major derangement to the PI3 kinase–AKT pathway downstream of ErbB receptors (Fig. 4 D). Interestingly, this also provides support for the view that the absence of FAK does not cause gross structural defects in laminin organization, as seen in the CNS (Beggs et al., 2003), because the absence of laminin from Schwann cell basal lamina causes major reductions in ErbB2 phosphorylation (Yu et al., 2005). Because the PI3 kinase pathway has been implicated in both cell survival and proliferation in Schwann cells (Li et al., 2001; Zanazzi et al., 2001), this demonstrates that the defect in proliferation during perinatal axonal sorting is not a result of deficits in FAK signaling via the PI3 kinase pathway. Furthermore, because AKT phosphorylation is unaffected during the active phase of perinatal Schwann cell proliferation, FAK does not appear to influence the signaling pathway from ErbB receptors via PI3 kinase to AKT, thus supporting the view that FAK acts via an independent pathway, probably originating with laminin. AKT may still be necessary to promote proliferation during radial sorting, but it is clearly not sufficient during radial sorting.

Although β1 integrin and FAK are functionally linked, Schwann cells lacking β1 integrin do not display reduced proliferation (Chen et al., 2000; Feltri et al., 2002). Nevertheless, ablation of these proteins can have distinct effects in the same cell type. FAK-null ES cells can differentiate, whereas the differentiation of β1 integrin–null ES cells is severely retarded (Andressen et al., 1998; Charlesworth et al., 2006). Furthermore, the fact that FAK can either suppress or promote growth in the same cell line indicates that diverse signaling pathways may have distinct roles to play in regulating proliferation at different stages of Schwann cell differentiation (Pirone et al., 2006).

Mutant nerves do not recover the ability to sort axons

In contrast to control nerves at 6 wk after birth, where axon ensheathment and the formation of a multilamellar compact myelin sheath were very advanced, mutant nerves still retained bundles of unsorted axons (Fig. 5, B and C). Typically, some axons that had been sorted to the edge of bundles were myelinated, but they were still attached to a bundle (Fig. 5 B), and some bundles appeared to be surrounded by fibroblasts (Fig. 5 C). There was no substantial progress in axon sorting up to 6 mo after birth, and bundles of large-caliber axons persisted with possible further evidence of perineurial fibroblast infiltration (Fig. 5 D). Hence, mutant nerves were unable to recover from the perinatal deficit in Schwann cells numbers.

Striking differences between control and mutant nerves were first demonstrable between E17.5 and E18.5, a time when Schwann cells normally increase in number by ~80%, whereas mutant cells increased by only 37%. We suggest that the impaired ability of FAK-null Schwann cells to proliferate during axon defasciculation contributes significantly to amyelination caused by an inadequate supply of Schwann cells. Although FAK has been shown to regulate proliferation in cultured cells, this is the first demonstration that it does so in vivo. Because the absence of FAK did not prevent insertion of Schwann cell processes into axon bundles, we propose that extension of cell processes between axons prefigures the mitotic stimulation of Schwann cells caused by contact with both axons and laminins. In future studies, it would be interesting to determine how the transduction pathways linked to the integrin and ErbB receptors regulate FAK and its downstream targets.

Materials and methods

Animals
All animal work conformed to UK legislation (Scientific Procedures) Act 1986 and the Edinburgh University Ethical Review policy. Generation of mice carrying targeted *lox*P sites in the *Fak* gene, and the genotyping of these mice, has been previously described (McLean et al., 2004). Targeted ablation of FAK in myelin-forming glia was achieved by crossing *Fak^{flox/flox}* mice with mice heterozygous both for the floxed allele and for *Cre* inserted into the *Cnp* locus (*Fak^{wt/flox}/Cnp-Cre*; Lappe-Siefke et al., 2003). Both *Fak^{flox/flox}* mice and heterozygous *Cnp-Cre* mice were phenotypically indistinguishable from wild-type mice, as previously shown (Lappe-Siefke et al., 2003; McLean et al., 2004). Cre-mediated recombination at E18.5 in sciatic nerves was assessed by PCR analysis of genomic DNA, followed by HindIII digestion, as previously described (McLean et al., 2004). Mean weights of newborn animals were measured using seven animals per condition.

Antibodies and microscopy
For Western blotting, we used anti-ErbB2 (1:250); anti–phospo-ErbB2 (Tyr877; 1:1,000); anti-AKT (1:1,000); and anti–phospho-AKT (Ser473; 1:1,000). All rabbit antibodies were obtained from Cell Signaling Technology, and a mouse monoclonal anti–β-actin (IgG1 clone AC-15) was purchased from Sigma-Aldrich. For immunofluorescence, we used rabbit anti-FAK obtained from UBI (BC3, 1:100) and Santa Cruz Biotechnology, Inc. (C-20, 1:50); mouse monoclonal anti–neurofilament-H purchased from Sigma-Aldrich (IgG$_1$ clone N32; 1:5,000); rabbit anti-activated caspase-3 (1:100) obtained from Cell Signaling Technology; and mouse monoclonal anti-BrdU clone B44 purchased from Becton Dickinson (IgG1; 1:6). Rabbit antibodies against Periaxin (Gillespie et al., 1994) and the neurofilament triplet proteins (Kelly et al., 1992) have been previously described. Nuclei were stained with either 0.1 μM TOTO-3 obtained from Invitrogen or 2 μM DAPI obtained from Sigma-Aldrich. Immunofluorescence labeling of cryostat sections have been previously described (Tait et al., 2000). Unless otherwise specified, all analyses were performed on the tibial branch of
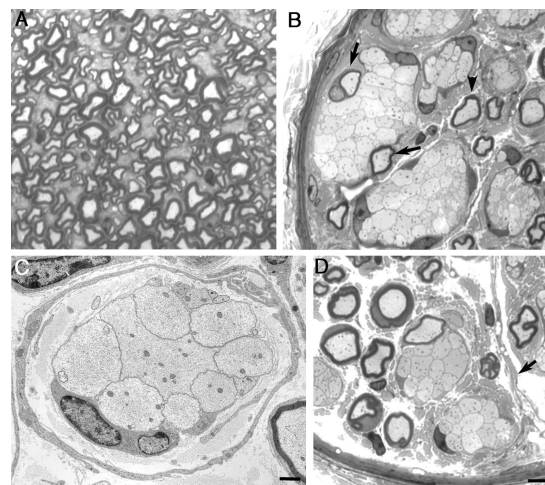

Figure 5. **Inefficient radial sorting in mutant nerves is irreversible.** (A) Light microscopy of 1-μm-thick transverse sections shows that wild-type sciatic nerves are extensively myelinated by 6 wk. (B) Light microscopy of mutant nerves reveals abundant bundles of unsorted axons, with some completely sorted axons (arrowhead) and some that have been partially sorted and myelinated at the periphery of bundles (arrow). (C) Electron microscopy shows that some of these bundles are enveloped by perineurial cells. (D) The bundles of large-caliber axons persist up to 6 mo after birth, with some evidence for further infiltration of perineurial fibroblasts (arrow). Bars: (A, B, and D) 5 μm; (C) 1 μm.

the sciatic nerve. We used a confocal microscope (TCL-SL; Leica) and Leica proprietary software. Conventional fluorescence microscopy was carried out using a microscope (BX60; Olympus), images were captured using a camera (Orca-ER; Hamamatsu), and morphometry was done with Openlab software (Improvision). Thin sections of nerves for electron microscopy were prepared as previously described (Gillespie et al., 2000). Photographic negatives were scanned and digitized. All figures were prepared using Photoshop version 7.0 (Adobe).

Cell counts
Timed-pregnant females (for E17.5 and 18.5 embryos) or individual pups (P2 and 4) were injected intraperitoneally or subcutaneously, respectively, with BrdU (100 μg/g body weight), and animals were killed by decapitation 70 min later. Nerves were fixed for 30 min in cold 4% paraformaldehyde and embedded in OCT; then 10-μm transverse sections were cut, and at least five sections per animal were counted. For Schwann cell quantitation, sections were stained with antineurofilament to identify nerves and with DAPI to identify cell nuclei. For BrdU labeling, rehydrated sections were treated with 0.5% Tween-20/PBS for 5 min, followed by a 1:1 mixture of 10 M HCl/0.5% Tween-20/PBS for 45 min. Sections were washed twice with PBS and twice with 0.5% Tween-20/PBS, and then coincubated with monoclonal anti-BrdU and rabbit antineurofilament antibodies for 2 h, followed by appropriate secondary antibodies. DAPI- or BrdU-labeled nuclei were only counted if they lay within the boundary of the neurofilament-positive tissue. The percentage of BrdU-positive nuclei was the mean BrdU count divided by the mean total cell count for that time point. Cross-sectional areas of 1 μm toluidine blue–stained sections of nerve, excluding the perineurium, were measured. The numbers of myelinated axons were quantitated in the same sections. For quantitation of the percentage of interdigitating Schwann cells, images were acquired for every axon bundle that had an associated Schwann cell with a distinct nucleus in a complete nerve section. A minimum of 30 Schwann cells was counted per sample.

Online supplemental material
10-wk-old wild-type (Video 1) and mutant (Video 2) mice were filmed to show the severe gait problems, especially in the hind limbs, displayed by demyelinated FAK-null mice. Online supplemental material available at http://www.jcb.org/cgi/content/full/jcb.200609021/DC1.

References

Andressen, C., S. Arnhold, M. Puschmann, W. Bloch, J. Hescheler, R. Fassler, and K. Addicks. 1998. Beta1 integrin deficiency impairs migration and differentiation of mouse embryonic stem cell derived neurons. *Neurosci. Lett.* 251:165–168.

Beggs, H.E., D. Schahin-Reed, K. Zang, S. Goebbels, K.A. Nave, J. Gorski, K.R. Jones, D. Sretavan, and L.F. Reichardt. 2003. FAK deficiency in cells contributing to the basal lamina results in cortical abnormalities resembling congenital muscular dystrophies. *Neuron.* 40:501–514.

Bunge, R.P., M.B. Bunge, and C.F. Eldridge. 1986. Linkage between axonal ensheathment and basal lamina production by Schwann cells. *Annu. Rev. Neurosci.* 9:305–328.

Charlesworth, P., N.H. Komiyama, and S.G. Grant. 2006. Homozygous mutation of focal adhesion kinase in embryonic stem cell derived neurons: normal electrophysiological and morphological properties in vitro. *BMC Neurosci.* 7:47.

Chen, L.M., D. Bailey, and C. Fernandez-Valle. 2000. Association of beta 1 integrin with focal adhesion kinase and paxillin in differentiating Schwann cells. *J. Neurosci.* 20:3776–3784.

Colognato, H., W. Baron, V. Avellana-Adalid, J.B. Relvas, A. Baron-Van Evercooren, E. Georges-Labouesse, and C. ffrench-Constant. 2002. CNS integrins switch growth factor signalling to promote target-dependent survival. *Nat Cell Biol.* 4:833–841.

Essayem, S., B. Kovacic-Milivojevic, C. Baumbusch, S. McDonagh, G. Dolganov, K. Howerton, N. Larocque, T. Mauro, A. Ramirez, D.M. Ramos, et al. 2006. Hair cycle and wound healing in mice with a keratinocyte-restricted deletion of FAK. *Oncogene.* 25:1081–1089.

Feltri, M.L., D. Graus Porta, S.C. Previtali, A. Nodari, B. Migliavacca, A. Cassetti, A. Littlewood-Evans, L.F. Reichardt, A. Messing, A. Quattrini, et al. 2002. Conditional disruption of β1 integrin in Schwann cells impedes interactions with axons. *J. Cell Biol.* 156:199–209.

Fernandez-Valle, C., L. Gwynn, P.M. Wood, S. Carbonetto, and M.B. Bunge. 1994. Anti-beta 1 integrin antibody inhibits Schwann cell myelination. *J. Neurobiol.* 25:1207–1226.

Fernandez-Valle, C., P.M. Wood, and M.B. Bunge. 1998. Localization of focal adhesion kinase in differentiating Schwann cell/neuron cultures. *Microsc. Res. Tech.* 41:416–430.

Geiger, B., A. Bershadsky, R. Pankov, and K.M. Yamada. 2001. Transmembrane crosstalk between the extracellular matrix–cytoskeleton crosstalk. *Nat. Rev. Mol. Cell Biol.* 2:793–805.

Gillespie, C.S., D.L. Sherman, G.E. Blair, and P.J. Brophy. 1994. Periaxin, a novel protein of myelinating Schwann cells with a possible role in axonal ensheathment. *Neuron.* 12:497–508.

Gillespie, C.S., D.L. Sherman, S.M. Fleetwood-Walker, D.F. Cottrell, S. Tait, E.M. Garry, V.C. Wallace, J. Ure, I.R. Griffiths, A. Smith, and P.J. Brophy. 2000. Peripheral demyelination and neuropathic pain behavior in periaxin-deficient mice. *Neuron.* 26:523–531.

Ilic, D., Y. Furuta, S. Kanazawa, N. Takeda, K. Sobue, N. Nakatsuji, S. Nomura, J. Fujimoto, M. Okada, and T. Yamamoto. 1995. Reduced cell motility and enhanced focal adhesion contact formation in cells from FAK-deficient mice. *Nature.* 377:539–544.

Ilic, D., C.H. Damsky, and T. Yamamoto. 1997. Focal adhesion kinase: at the crossroads of signal transduction. *J. Cell Sci.* 110:401–407.

Jessen, K.R., and R. Mirsky. 2005. The origin and development of glial cells in peripheral nerves. *Nat. Rev. Neurosci.* 6:671–682.

Kelly, B.M., C.S. Gillespie, D.L. Sherman, and P.J. Brophy. 1992. Schwann cells of the myelin-forming phenotype express neurofilament protein NF-M. *J. Cell Biol.* 118:397–410.

Lappe-Siefke, C., S. Goebbels, M. Gravel, E. Nicksch, J. Lee, P.E. Braun, I.R. Griffiths, and K.A. Nave. 2003. Disruption of Cnp1 uncouples oligo-dendroglial functions in axonal support and myelination. *Nat. Genet.* 33:366–374.

Li, Y., G.I. Tennekoon, M. Birnbaum, M.A. Marchionni, and J.L. Rutkowski. 2001. Neuregulin signaling through a PI3K/Akt/Bad pathway in Schwann cell survival. *Mol. Cell. Neurosci.* 17:761–767.

Martin, J.R., and H.D. Webster. 1973. Mitotic Schwann cells in developing nerve: their changes in shape, fine structure, and axon relationships. *Dev. Biol.* 32:417–431.

McLean, G.W., N.H. Komiyama, B. Serrels, H. Asano, L. Reynolds, F. Conti, K. Hodivala-Dilke, D. Metzger, P. Chambon, S.G. Grant, and M.C. Frame. 2004. Specific deletion of focal adhesion kinase suppresses tumor formation and blocks malignant progression. *Genes Dev.* 18:2998–3003.

Michailov, G.V., M.W. Sereda, B.G. Brinkmann, T.M. Fischer, B. Haug, C. Birchmeier, L. Role, C. Lai, M.H. Schwab, and K.A. Nave. 2004. Axonal neuregulin-1 regulates myelin sheath thickness. *Science.* 304:700–703.

Morrissey, T.K., A.D. Levi, A. Nuijens, M.X. Sliwkowski, and R.P. Bunge. 1995. Axon-induced mitogenesis of human Schwann cells involves heregulin and p185erbB2. *Proc. Natl. Acad. Sci. USA.* 92:1431–1435.

Pirone, D.M., W.F. Liu, S.A. Ruiz, L. Gao, S. Raghavan, C.A. Lemmon, L.H. Romer, and C.S. Chen. 2006. An inhibitory role for FAK in regulating proliferation: a link between limited adhesion and RhoA-ROCK signaling. *J. Cell Biol.* 174:277–288.

Previtali, S.C., A. Nodari, C. Taveggia, C. Pardini, G. Dina, A. Villa, L. Wrabetz, A. Quattrini, and M.L. Feltri. 2003. Expression of laminin receptors in Schwann cell differentiation: evidence for distinct roles. *J. Neurosci.* 23:5520–5530.

Riethmacher, D., E. Sonnenberg-Riethmacher, V. Brinkmann, T. Yamaai, G.R. Lewin, and C. Birchmeier. 1997. Severe neuropathies in mice with targeted mutations in the ErbB3 receptor. *Nature.* 389:725–730.

Salzer, J.L., A.K. Williams, L. Glaser, and R.P. Bunge. 1980. Studies of Schwann cell proliferation. II. Characterization of the stimulation and specificity of the response to a neurite membrane fraction. *J. Cell Biol.* 84:753–766.

Sherman, D.L., and P.J. Brophy. 2000. A tripartite nuclear localization signal in the PDZ-domain protein L-periaxin. *J. Biol. Chem.* 275:4537–4540.

Sherman, D.L., and P.J. Brophy. 2005. Mechanisms of axon ensheathment and myelin growth. *Nat. Rev. Neurosci.* 6:683–690.

Stewart, H.J., L. Morgan, K.R. Jessen, and R. Mirsky. 1993. Changes in DNA synthesis rate in the Schwann cell lineage in vivo are correlated with the precursor–Schwann cell transition and myelination. *Eur. J. Neurosci.* 5:1136–1144.

Tait, S., F. Gunn-Moore, J.M. Collinson, J. Huang, C. Lubetzki, L. Pedraza, D.L. Sherman, D.R. Colman, and P.J. Brophy. 2000. An oligodendrocyte cell adhesion molecule at the site of assembly of the paranodal axo-glial junction. *J. Cell Biol.* 150:657–666.

Taveggia, C., G. Zanazzi, A. Petrylak, H. Yano, J. Rosenbluth, S. Einheber, X. Xu, R.M. Esper, J.A. Loeb, P. Shrager, et al. 2005. Neuregulin-1 type III determines the ensheathment fate of axons. *Neuron.* 47:681–694.

Vartanian, T., A. Goodearl, S. Lefebvre, S.K. Park, and G. Fischbach. 2000. Neuregulin induces the rapid association of focal adhesion kinase with the erbB2-erbB3 receptor complex in Schwann cells. *Biochem. Biophys. Res. Commun.* 271:414–417.

Wallquist, W., S. Plantman, S. Thams, J. Thyboll, J. Kortesmaa, J. Lannergren, A. Domogatskaya, S.O. Ogren, M. Risling, H. Hammarberg, et al. 2005. Impeded interaction between Schwann cells and axons in the absence of laminin alpha4. *J. Neurosci.* 25:3692–3700.

Webster, H.D., R. Martin, and M.F. O'Connell. 1973. The relationships between interphase Schwann cells and axons before myelination: a quantitative electron microscopic study. *Dev. Biol.* 32:401–416.

Wood, P.M., and R.P. Bunge. 1975. Evidence that sensory axons are mitogenic for Schwann cells. *Nature.* 256:662–664.

Yang, D., J. Bierman, Y.S. Tarumi, Y.P. Zhong, R. Rangwala, T.M. Proctor, Y. Miyagoe-Suzuki, S. Takeda, J.H. Miner, L.S. Sherman, et al. 2005. Coordinate control of axon defasciculation and myelination by laminin-2 and -8. *J. Cell Biol.* 168:655–666.

Yu, W.M., M.L. Feltri, L. Wrabetz, S. Strickland, and Z.L. Chen. 2005. Schwann cell-specific ablation of laminin gamma1 causes apoptosis and prevents proliferation. *J. Neurosci.* 25:4463–4472.

Yuan, X., R. Chittajallu, S. Belachew, S. Anderson, C.J. McBain, and V. Gallo. 2002. Expression of the green fluorescent protein in the oligodendrocyte lineage: a transgenic mouse for developmental and physiological studies. *J. Neurosci. Res.* 70:529–545.

Zanazzi, G., S. Einheber, R. Westreich, M.J. Hannocks, D. Bedell-Hogan, M.A. Marchionni, and J.L. Salzer. 2001. Glial growth factor/neuregulin inhibits Schwann cell myelination and induces demyelination. *J. Cell Biol.* 152:1289–1299.